

Collaborative Optimization of Battery Charging / Swapping Stations for eVTOLs Based on Closed-Loop Supply Chain and Space-Time Network

Pengfeng Lin^{1*}, Miao Zhu¹, Jiahui Sun², Haoyang Cui², Xiaoyong Cao¹, Chuanlin Zhang², Yunda Yan³

¹ Faculty of Artificial Intelligence, Shanghai University of Electric Power, Shanghai 201306, China

² School of Electrical Engineering, Shanghai Jiao Tong University, Shanghai 200240, China

³ Department of Computer Science, University College London, London WC1E 6BT, UK

* linpengfeng@iceee.org

Keywords: Electric vertical take-off and landing, Closed-loop supply chain, Time-space network, Battery logistics.

Abstract: Against the backdrop of the burgeoning global low-altitude economy, countries have successively introduced a series of policies to accelerate the application and commercialization of electric vertical take-off and landing (eVTOL) aircraft. Nevertheless, purely electric eVTOLs confront constraints including limited battery energy density, high operational power requirements, and challenges associated with rapid energy replenishment, which collectively restrict their flight endurance and application scenarios. Furthermore, while eVTOL deployment is scaling up, supporting charging infrastructure and regulations remain underdeveloped. This situation presents emerging power distribution networks with new challenges in maintaining adequate electricity supply and ensuring operational continuity. To tackle these issues, following an investigation into battery energy replenishment strategies, a closed-loop supply chain-based model for eVTOL battery charging and swapping is proposed. Time-space network methods are utilized to characterize the scheduling of batteries and logistics throughout the system. Subsequently, aiming to maximize the operational revenue of the model, optimized management of battery swapping, transportation, and charging processes is implemented, facilitating coordinated operation among eVTOLs, swapping stations, and charging stations. Finally, the model is solved by Gurobi, verifying its feasibility. Simulation results further indicate that the model alleviates range anxiety for eVTOLs, offering strong support for their commercialization. Moreover, it enables coordinated scheduling between eVTOLs and the distribution network, thereby facilitating the network's gradual improvement and upgrading.

I. INTRODUCTION

In China, with policies such as the "National Comprehensive Three-Dimensional Transportation Network Plan Outline" listing the low-altitude economy as a key development target, electric Vertical Take-off and Landing (eVTOL) aircraft have garnered widespread attention from local governments and high-tech enterprises due to their advantages such as low

emissions, low noise, and point-to-point direct transportation. As eVTOLs do not occupy ground roads and can be applied to various scenarios including short-distance transport and medical rescue, their demand is particularly significant in densely populated and congested metropolitan areas. In the current construction of comprehensive transportation hubs centered on Shanghai Pudong Airport and the Shanghai East Railway

Station, the Standing Committee of the Shanghai Municipal Committee of the Chinese People's Political Consultative Conference has proposed the introduction of eVTOLs as a new mode of transportation^[1]. Concurrently, companies like AutoFlight have taken the lead in the mass production of eVTOLs, demonstrating strong capabilities to lead in this field. Furthermore, Morgan Stanley predicts that the global market value of eVTOLs will reach as high as 1.5 trillion US dollars by 2040, with China being the largest application market globally^[2]. Nevertheless, despite robust policy support, a solid industrial foundation, and broad development prospects, key issues remain to be addressed for the widespread adoption of eVTOLs.

Purely electric eVTOLs face challenges such as insufficient battery energy density, high operational power demand^[3], and difficulties in rapid energy replenishment, which severely constrain their range and application scenarios. Currently, the highest level of eVTOL battery energy density is around 300 Wh/kg, still significantly below the ideal target of 400 Wh/kg. Meanwhile, the discharge rate and peak power duration required during take-off and landing far exceed those of electric vehicles, preventing eVTOLs from meeting the demands of long-distance transport^[4-5]. Furthermore, profitability for eVTOLs depends on a high-turnover operational model, which necessitates frequent take-offs and landings. However, current fast-charging technologies are unable to achieve deep battery replenishment within a short time^[6-8], directly limiting the daily number of flight cycles and overall operational efficiency. Therefore, to promote the application and development of eVTOLs, it is essential to study rapid energy replenishment solutions for their batteries.

Plug-in charging, as one of the energy replenishment methods for eVTOLs, has prompted scholars to propose various charging scheduling strategies based on different optimization objectives. Reference[9] investigated the eVTOL charging sequencing and scheduling problem, designing a charging plan that simultaneously meets eVTOL charging demands and minimizes customer waiting time. The joint scheduling method in Reference[10] can generate optimal travel routes and

charging tasks for each aircraft based on charging station capacity, aircraft state of charge, and logistics requirements. Reference[11] first formulated the eVTOL scheduling plan and feasible charging schedule according to travel demand, then optimized the charging time and rate considering grid dynamics to maximize power system benefits.

In addition to plug-in charging, battery swapping is another energy replenishment method for eVTOLs^[12]. Given current practical constraints, the battery swapping strategy holds significant advantages. Current fast-charging technology for eVTOL batteries struggles to complete charging within 5–10 minutes^[4-5], severely reducing operational efficiency. Moreover, the heat generated during fast charging can accelerate battery capacity degradation and shorten lifespan^[13]. In contrast, the entire battery swapping process requires minimal time, ensuring high operational efficiency. Furthermore, batteries are not subjected to sustained high loads or excessive heat generation^[7], effectively extending their service life. Additionally, reference[12] demonstrates that adopting a battery swapping strategy can more readily reduce operational costs.

In the field of electric vehicles, some scholars have proposed an operational model for the battery swapping strategy^[14], where the Battery Swapping Station (BSS) is solely responsible for all operations including battery charging, swapping, and auxiliary services. However, directly charging the depleted batteries (DB) at the BSS complicates its structure^[15]. Additionally, it requires substantial space for charging facilities and battery storage, significantly increasing construction costs.

Charging DBs centrally at a Battery Charging Station (BCS) can avoid the aforementioned drawbacks. Therefore, some scholars have proposed an improved battery charging-swapping system (BCSS) model, where the BSSs solely provide battery swapping services, and the BCSs centrally charge the swapped-out DBs. To ensure coordinated operation between the BCSs and BSSs, the battery logistics system connecting them is also critical. Reference[16] proposed a battery scheduling framework; however, this study primarily focused on optimal

route planning and did not sufficiently address the operational management of the BCSs and BSSs. In summary, when researching charging-swapping strategies for eVTOLs, it is essential to coordinate the BSSs, logistics system, and BCSs comprehensively to maximize the operational revenue of the entire system.

In light of this, this paper proposes a battery charging-swapping system model for eVTOLs based on a closed-loop supply chain (CLSC). First, a CLSC model tailored to the operational characteristics of eVTOLs, BSSs, and BCSs is constructed. Subsequently, the scheduling of batteries and logistics within the model is described using time-space network (TSN) techniques. Then, under the premise of meeting the battery swapping demands of eVTOLs, the swapping, transportation, and charging of batteries within the model are optimized. This achieves joint operation among eVTOLs, BSSs, and BCSs and maximizes the operational revenue of the entire system. Finally, the simulation is conducted to verify the feasibility of the proposed model. To the best of our knowledge, this research addresses a gap in the joint operation and management of eVTOLs, BSSs, and BCSs, providing a theoretical foundation and methodological support for the realization of integrated ground-air systems.

II. MODELING AND OPERATIONAL PRINCIPLES OF THE eVTOL BATTERY CHARGING AND SWAPPING SYSTEM

This section selects a suitable CLSC model by analyzing the characteristics of each member in the BCSS. Subsequently, a model of the eVTOL battery charging and swapping system based on the selected CLSC model is constructed, and its working principle is elaborated.

A. Closed-Loop Supply Chain Model Selection

As a management model for achieving resource recycling^[17], CLSC has been applied in various fields. For example, in the field of electric vehicle battery recycling, literature[18] effectively coordinated various participants and improved overall economic benefits by designing control strategies for CLSC models, while also reducing the environmental impact of

batteries. In the area of logistics transportation optimization, literature[19] addressed the vehicle routing problem involving pick-up and delivery within CLSC under the premise of meeting uncertain demand. Despite the universal applicability of CLSC and the multiple benefits it can bring, no research has yet been found applying it to the field of eVTOL battery energy replenishment.

After analyzing the functions of each member in the BCSS, three trade-in CLSC models^[17] are available for selection. In Model R, retailers wholesale new products from manufacturers and sell them to consumers, while used products are returned by consumers to retailers and then sent back to the manufacturers. In Model C, manufacturers and retailers are integrated into a single enterprise, selling products directly to consumers while simultaneously recovering used products. Model M differs from Model R in that used products are recovered directly by manufacturers from consumers. In the BCSS, Model C is suitable for scenarios where the BSS can handle all operations, while Model M applies when eVTOLs directly exchange batteries with the BCS. Since the scenario described in this paper does not align with the conditions of the two aforementioned models, Model R is adopted as the CLSC model.

B. Working Principle of the eVTOL Battery Charging and Swapping System Model Based on CLSC

The overall structure of the BCSS based on Model R proposed in this paper is shown in Fig. 1, which consists of eVTOLs, BSSs, a BCS, and a truck transportation fleet. As comprehensive service points, BSSs provide battery swapping services for eVTOLs and also serve as passenger transfer and waiting points. The BCS charges DBs and supplies well-charged batteries(WB) to BSSs. The truck transportation fleet transports batteries between them, delivering WBs from the BCS to BSSs and collecting DBs from BSSs for return to the BCS. Consequently, eVTOLs, BSSs, and the BCS correspond to the customers, retailers, and manufacturer in Model R, respectively, while the truck fleet connects retailers and the manufacturer. For convenience of discussion, this paper establishes eight

assumptions regarding the proposed BCSS, described in detail as follows:

(1) All eVTOL batteries are of the same model, specifically designed for the daily operation of Airbus's CityAirbus.

(2) All DBs have the same minimum state of charge (SOC_{min}), and all WBs have the same maximum state of charge (SOC_{max}).

(3) The BCS in the system purchases electricity from the power grid at prices set by the grid operator.

(4) The BCS is equipped with a certain number of charging piles, but this number is less than the total quantity of batteries in the BCSS. Once fully charged, batteries must be removed from the charging piles and stored in the BCS warehouse. Additionally, the BCS reserves space for storing DBs.

(5) The BCS can lease backup DBs from a third-party company at a cost if its battery supply is insufficient.

(6) When the DB inventory at a BCS exceeds the number of available charging piles, batteries are randomly selected from the DB inventory for charging in subsequent time steps. There is no need to lease backup DBs, nor is it required to follow a first-in-first-out charging sequence.

(7) The total supply of WBs from the BCS can meet the battery swapping service demand of all BSSs.

(8) To ensure the service quality of battery swapping at BSSs, each BSS maintains a reserve inventory of both WBs and DBs.

Taking Shanghai as an example, three BSSs, one BCS, and a transportation fleet consisting of four trucks are deployed within the city, as shown in Fig. 1. Thanks to the initial WB inventory, the BSS on Chongming Island can provide immediate battery swapping services to arriving eVTOLs without waiting for incoming trucks. At the BSS in downtown Shanghai, a truck is unloading WBs and loading DBs while the station simultaneously performs battery swaps for an eVTOL. At the BSS located at the border of Qingpu District and Songjiang District, following replenishment and clearance by trucks, the

WB inventory is sufficient, and only DBs generated from the current swap operation remain on-site. Meanwhile, the BCS in Fengxian District, serving as the system's charging hub, is simultaneously handling battery charging, truck loading, and unloading tasks to ensure the stable operation of the battery logistics system.

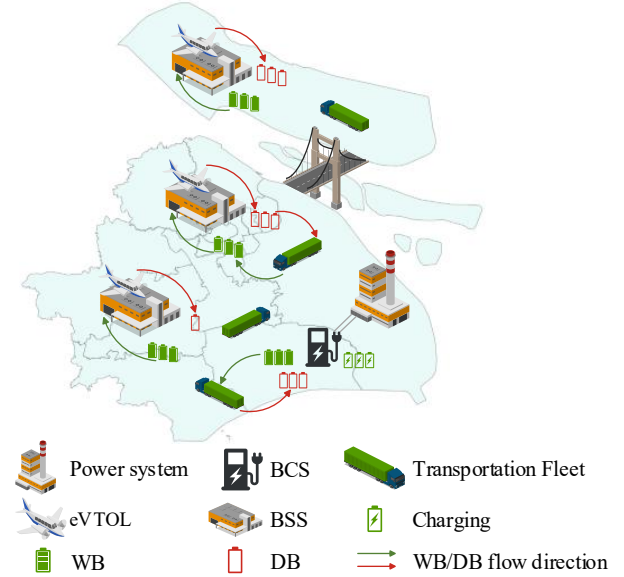


Fig. 1. CLSC-based charging and swapping system for eVTOL batteries(taking Shanghai city as an example) .

III. OPTIMAL OPERATION MANAGEMENT FOR THE CLSC-BASED EVTOL BATTERY CHARGING AND SWAPPING SYSTEM

Based on the BCSS described in the previous section and the scenario illustrated in Fig. 1, this section establishes operational models for the logistics system, BSSs, and BCS, respectively, and presents their corresponding objective functions.

A. Logistics System Operation Model Based on TSN

The TSN is easy to model and solve when handling time-series-related problems and is therefore commonly used to address operational issues in the aviation and power system domains^[20-23]. This paper constructs a battery charging and swapping system model that integrates eVTOL battery operations, urban traffic dispatch, and power system regulation. To address the scheduling optimization problem for trucks and

eVTOL batteries within this system, this section proposes a logistics system operational model based on TSN.

1) Vehicle Scheduling and Battery Scheduling Models

As shown in Fig. 2(a), the BCSS comprises one BCS and three BSSs, corresponding to nodes 1-4 respectively, and is interconnected via a transportation network. Each edge in the network is labeled with the number of time steps required for a truck to travel from one node to another. For instance, traveling from the BCS to BSS1 requires one time step. For nodes in the network that are connected but have a travel time greater than one time step, introducing virtual nodes between them ensures that the distance between all nodes in the network is one time step, thereby guaranteeing a defined state for each edge at every time step. As illustrated in Fig. 2(b), this paper introduces a virtual node5 between the BCS and BSS2.

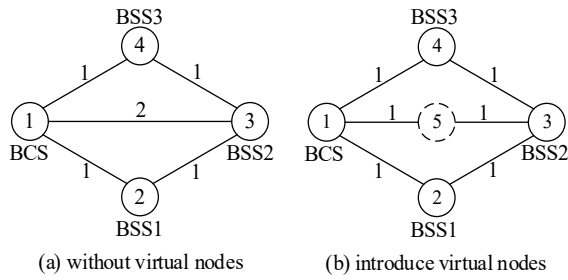


Fig. 2. Transportation network of BCSS.

In Fig. 3, the transportation network is modeled as a TSN, consisting of time steps, nodes, and arcs representing travel paths. Node1 is the BCS, nodes 2-4 correspond to BSS1-BSS3, and node5 is the virtual node. Two types of arcs are used to represent truck parking and travel behaviors, respectively. For instance, an arc connecting the same node across consecutive time steps is a parking arc, indicating the truck is parked at that node. An arc connecting different nodes across consecutive time steps is a travel arc, indicating the truck is traveling on that route. Furthermore, there are no parking arcs at the virtual node. Using the TSN, the BCSS can track the state, location, and task of any truck at each time step, thereby enabling optimal scheduling of the logistics system based on the battery swapping demand of eVTOLs.

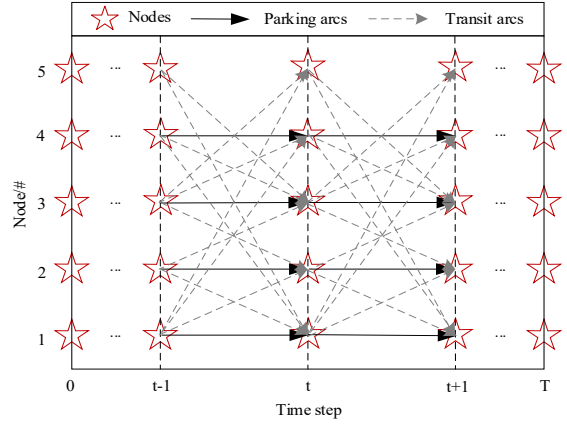


Fig. 3. Logistics system operation model based on TSN.

The operational model for the logistics system proposed in this paper comprises a vehicle scheduling model and a battery scheduling model for each truck. The vehicle scheduling model is presented in Equations (1)-(4).

The real-time status of each truck serves as a critical basis for the BCSS to assign tasks for the next time step. Therefore, it must be ensured that a truck can only be in either a "traveling" or "parked" state at any given time step:

$$\sum_{(i,j) \in Z} \zeta_{arc,(i,j)}^{\omega,t} = 1, \forall \omega \in H, t \in \mathcal{T} \quad (1)$$

In the formula: $\zeta_{arc,(i,j)}^{\omega,t}$ is a binary variable. If truck ω is on the arc starting from node i and heading to node j at time step t , the value of this variable is 1; Z is the set of all arcs in the TSN; (i, j) represents the arc with i as the start node and j as the end node; H is the set of all trucks; ω represents the identification number of each truck; \mathcal{T} is the set of all time steps; t denotes each time step.

This paper sets that truck ω is located at node i at the initial moment and can only depart from this node at time step 1. Therefore, we have:

$$\sum_{(i,j) \in Z_i^+} \zeta_{arc,(i,j)}^{\omega,1} = \zeta_{arc,i}^{\omega,ini}, \forall \omega \in H, i, j \in G_R \cup G_V \quad (2)$$

In the formula: Z_i^+ is the set of arcs starting from node i ; G_R is the set of actual nodes; G_V is the set of virtual nodes.

To prevent trucks from disappearing or appearing arbitrarily, continuity must be ensured in their scheduling between nodes. If the destination node of a truck at time step t is j , then its departure node at time step $t+1$ must also be j :

$$\sum_{(i,j) \in Z_j^-} \zeta_{\text{arc},(i,j)}^{\omega,t} = \sum_{(j,k) \in Z_j^+} \zeta_{\text{arc},(j,k)}^{\omega,t+1}, \forall \omega \in H, \quad (3)$$

$$i, j, k \in G_R \cup G_V, t \in \mathcal{T} \setminus \{T\}$$

In the formula: Z_j^- is the set of arcs ending at node j ; T represents the last time step.

However, to accurately calculate the total scheduling cost of the logistics system and further optimize the scheduling strategy, the BCSS must also track the specific state of each truck. Therefore, the truck transportation state variable is defined:

$$\beta_{\text{tru_on}}^{\omega,t} = \sum_{(i,j) \in Z, i \neq j} \zeta_{\text{arc},(i,j)}^{\omega,t}, \forall \omega \in H, i, j \in G_R \cup G_V, t \in \mathcal{T} \quad (4)$$

In the formula: $\beta_{\text{tru_on}}^{\omega,t}$ is a binary variable, if the departure node and the destination node of truck ω at time step t are different, this variable equals 1, indicating the truck is in a traveling state; otherwise, it equals 0.

Building upon the vehicle scheduling model, the battery scheduling model for each truck is jointly defined by Equations (5)-(15). Specifically, the expression for the quantity of DBs carried by each truck at each time step is:

$$S_{\text{tru,DB,stor}}^{\omega,t} = \begin{cases} \sum_{n \in G_{\text{BSS}}} N_{\text{tru,BSS,DB}}^{\omega,n,t} - \sum_{m \in G_{\text{BCS}}} N_{\text{tru,BCS,DB}}^{\omega,m,t}, \forall \omega \in H, t = 1 \\ S_{\text{tru,DB,stor}}^{\omega,t-1} + \sum_{n \in G_{\text{BSS}}} N_{\text{tru,BSS,DB}}^{\omega,n,t} - \sum_{m \in G_{\text{BCS}}} N_{\text{tru,BCS,DB}}^{\omega,m,t}, \forall \omega \in H, t \in \mathcal{T} \setminus \{1\} \end{cases} \quad (5)$$

In the formula: $S_{\text{tru,DB,stor}}^{\omega,t}$ is the number of DBs carried by the truck ω at time step t ; $N_{\text{tru,BSS,DB}}^{\omega,n,t}$ is the number of DBs loaded at BSS n ; $N_{\text{tru,BCS,DB}}^{\omega,m,t}$ is the number of DBs unloaded at BCS m ; G_{BSS} is the set of BSSs; n is the index of its elements; G_{BCS} is the set of BCSs; m is the index of its elements.

Similarly, the expression for the number of WBs, denoted as $S_{\text{tru,WB,stor}}^{\omega,t}$, carried by the truck at each time step is:

$$S_{\text{tru,WB,stor}}^{\omega,t} = \begin{cases} \sum_{m \in G_{\text{BCS}}} N_{\text{tru,BCS,WB}}^{\omega,m,t} - \sum_{n \in G_{\text{BSS}}} N_{\text{tru,BSS,WB}}^{\omega,n,t}, \forall \omega \in H, t = 1 \\ S_{\text{tru,WB,stor}}^{\omega,t-1} + \sum_{m \in G_{\text{BCS}}} N_{\text{tru,BCS,WB}}^{\omega,m,t} - \sum_{n \in G_{\text{BSS}}} N_{\text{tru,BSS,WB}}^{\omega,n,t}, \forall \omega \in H, t \in \mathcal{T} \setminus \{1\} \end{cases} \quad (6)$$

In the formula: $N_{\text{tru,BCS,WB}}^{\omega,m,t}$ is the number of WBs loaded by the truck at BCS m at time step t ; $N_{\text{tru,BSS,WB}}^{\omega,n,t}$ is the number of WBs unloaded by the truck at BSS n at time step t .

For the decision variables involved in Equations (5) and (6), their ranges must be constrained to avoid violating basic physical principles. For instance, the total number of DBs and WBs carried by a truck cannot exceed its maximum transportation capacity:

$$S_{\text{tru,DB,stor}}^{\omega,t} + S_{\text{tru,WB,stor}}^{\omega,t} \leq C_{\text{tru,cap}}, \forall \omega \in H, t \in \mathcal{T} \quad (7)$$

In the formula: $C_{\text{tru,cap}}$ is the maximum number of batteries that can be carried by a truck.

Furthermore, constraints must be applied to the quantities of DBs and WBs carried by the truck. For example, it must be ensured that both quantities are non-negative integers and always remain within a reasonable range. Additionally, this paper stipulates that at the end of each time step, the remaining quantities of WBs and DBs on the truck cannot exceed one-third of the maximum capacity. These requirements are implemented by Equations (8) and (9), respectively:

$$\begin{cases} 0 \leq S_{\text{tru,DB,stor}}^{\omega,t} \leq C_{\text{tru,cap}}, \forall \omega \in H, t \in \mathcal{T} \\ 0 \leq S_{\text{tru,WB,stor}}^{\omega,t} \leq C_{\text{tru,cap}}, \forall \omega \in H, t \in \mathcal{T} \end{cases} \quad (8)$$

$$\begin{cases} S_{\text{tru,DB,stor}}^{\omega,T} \leq C_{\text{tru,cap}} / 3, \forall \omega \in H \\ S_{\text{tru,WB,stor}}^{\omega,T} \leq C_{\text{tru,cap}} / 3, \forall \omega \in H \end{cases} \quad (9)$$

The prerequisite for a truck to load DBs at a BSS is that it must be docked at that BSS, and the loading quantity cannot exceed its transport capacity:

$$0 \leq N_{\text{tru,BSS,DB}}^{\omega,n,t} \leq C_{\text{tru,cap}} \zeta_{\text{arc},(n,n)}^{\omega,t}, \forall \omega \in H, \forall n \in G_{\text{BSS}}, t \in \mathcal{T} \quad (10)$$

When a truck unloads WBs at a BSS, it must adhere to the following constraints. Equation (11) requires that unloading can only occur when the truck is parked. Equation (12) stipulates

that no WBs can be unloaded at time step1, and at other time steps, the number unloaded cannot exceed the quantity of WBs carried by the truck at the previous time step:

$$0 \leq N_{\text{tru,BSS,WB}}^{\omega,n,t} \leq C_{\text{tru,cap}} \zeta_{\text{arc,(n,n)}}, \forall \omega \in H, \forall n \in G_{\text{BSS}}, t \in \mathcal{T} \quad (11)$$

$$\left. \begin{aligned} N_{\text{tru,BSS,WB}}^{\omega,n,t} &= 0, \forall \omega \in H, \forall n \in G_{\text{BSS}}, t = 1 \\ N_{\text{tru,BSS,WB}}^{\omega,n,t} &\leq S_{\text{tru,WB,stor}}^{\omega,t-1}, \forall \omega \in H, \forall n \in G_{\text{BSS}}, t \in \mathcal{T} \setminus \{1\} \end{aligned} \right\} \quad (12)$$

Similarly, the loading of WBs and unloading of DBs by trucks at the BCS can be achieved using (13) to (15).

$$0 \leq N_{\text{tru,BCS,WB}}^{\omega,m,t} \leq C_{\text{tru,cap}} \zeta_{\text{arc,(m,m)}}, \forall \omega \in H, \forall m \in G_{\text{BCS}}, t \in \mathcal{T} \quad (13)$$

$$0 \leq N_{\text{tru,BCS,DB}}^{\omega,m,t} \leq C_{\text{tru,cap}} \zeta_{\text{arc,(m,m)}}, \forall \omega \in H, \forall m \in G_{\text{BSS}}, t \in \mathcal{T} \quad (14)$$

$$\left. \begin{aligned} N_{\text{tru,BCS,DB}}^{\omega,m,t} &= 0, \forall \omega \in H, \forall m \in G_{\text{BCS}}, t = 1 \\ N_{\text{tru,BCS,DB}}^{\omega,m,t} &\leq S_{\text{tru,DB,stor}}^{\omega,t-1}, \forall \omega \in H, \forall m \in G_{\text{BCS}}, t \in \mathcal{T} \setminus \{1\} \end{aligned} \right\} \quad (15)$$

2) Objective Function of the Logistics System Operation Model

This paper aims to maximize the operational revenue of the logistics system by optimizing the scheduling of trucks and batteries within it, while considering the eVTOL battery swapping demand at BSSs and the battery supply capacity of the BCS. Accordingly, the following objective function for the logistics system operation is presented:

$$\begin{aligned} \max P_{\text{obj,tran}} &= \sum_{t=1}^T \left[-\lambda_{\text{tru,tran}} \sum_{\omega \in H} \beta_{\text{tru,on}}^{\omega,t} \right. \\ &- \lambda_{\text{labor}} \sum_{m \in G_{\text{BCS}}} \sum_{\omega \in H} (N_{\text{tru,BCS,DB}}^{\omega,m,t} + N_{\text{tru,BCS,WB}}^{\omega,m,t}) \\ &\left. - \lambda_{\text{labor}} \sum_{n \in G_{\text{BSS}}} \sum_{\omega \in H} (N_{\text{tru,BSS,DB}}^{\omega,n,t} + N_{\text{tru,BSS,WB}}^{\omega,n,t}) \right] \quad (16) \end{aligned}$$

In the formula: the first term represents the total transportation cost incurred by the logistics system scheduling; $\lambda_{\text{tru,tran}}$ is the transportation fee for a truck traveling for one time step; the second and third terms are the manual handling costs for loading and unloading batteries at the BCS and BSSs, respectively, and λ_{labor} is the handling cost for a single battery.

B. BSS Operation Model

1) Modeling Principles and Battery Swapping Service Constraints for BSS

This paper models the operation of the BSS as comprising a queue of eVTOLs awaiting battery swapping, a DB inventory, and a WB inventory. To facilitate the analysis of the BSSs' battery swapping service performance, the discrete cumulative curve method is adopted, modeling the eVTOL queue as the arrival and departure of battery packs^[24]. Specifically, the arrival curve is defined as $A^{n,t}$, describing the cumulative number of battery swapping services that BSS n is required to provide from time step1 to t . The departure curve is defined as $D^{n,t}$, recording the cumulative number of battery swapping services that BSS n has actually provided from time step1 to t . Additionally, to prevent passenger waiting times from being unreasonably extended, a minimum departure curve $D_{\text{min}}^{n,t}$ is introduced into the model, which specifies the minimum cumulative number of battery swapping services that BSS n must have completed by the current time step. Assuming there are two CityAirbus aircraft, each with 4 batteries, where CityAirbus1 arrives at BSS n at time step t and can accept departure from the BSS no later than time step $t+2$, and CityAirbus2 arrives at BSS n at time step $t+1$ and can accept departure from the BSS no later than time step $t+3$, then $A^{n,t} = 4$, $D_{\text{min}}^{n,t+2} = 4$, $A^{n,t+1} = 8$, $D_{\text{min}}^{n,t+3} = 8$.

In summary, the BSS must adhere to the following battery swapping service constraints. First, the $D^{n,t}$ of any BSS at any time step cannot exceed the $A^{n,t}$ of that BSS. Second, to balance the operational revenue of the BCSS and passenger waiting times, the $D^{n,t}$ at each time step must not fall below the specified $D_{\text{min}}^{n,t}$:

$$D_{\text{min}}^{n,t} \leq D^{n,t} \leq A^{n,t}, n \in G_{\text{BSS}}, t \in \mathcal{T} \quad (17)$$

The second battery swapping service constraint is shown in Equation (18), which serves as a necessary supplement to

Equation (17) to ensure that $D^{n,t}$ either increases or remains constant as time steps progress:

$$D^{n,t-1} \leq D^{n,t}, n \in G_{\text{BSS}}, t \in \mathcal{T} \setminus \{1\} \quad (18)$$

2) BSS Battery Dynamic Inventory Model

During its daily operations, the BSS interacts with the logistics system and eVTOLs for battery exchanges, causing real-time changes in its WB and DB inventories. Accordingly, this section constructs a BSS battery dynamic inventory model as shown in Equations (19)-(25).

The BCSS deeply couples the BSS with the logistics system through battery loading, unloading, and transportation. $N_{\text{BSS,DB,sup}}^{n,t}$ and $N_{\text{BSS,WB,rec}}^{n,t}$, as defined by Equations (19) and (20), represent the quantity of DBs provided by BSS n to the logistics system and the quantity of WBs received by BSS n from the logistics system at time step t , respectively:

$$N_{\text{BSS,DB,sup}}^{n,t} = \sum_{\omega} N_{\text{tru,BSS,DB}}^{\omega,n,t}, \forall \omega \in H, \forall n \in G_{\text{BSS}}, t \in \mathcal{T} \quad (19)$$

$$N_{\text{BSS,WB,rec}}^{n,t} = \sum_{\omega} N_{\text{tru,BSS,WB}}^{\omega,n,t}, \forall \omega \in H, \forall n \in G_{\text{BSS}}, t \in \mathcal{T} \quad (20)$$

Furthermore, the DB and WB inventory of BSS n at time step t , namely $S_{\text{BSS,DB,stor}}^{n,t}$ and $S_{\text{BSS,WB,stor}}^{n,t}$, can be defined by the following expressions:

$$S_{\text{BSS,DB,stor}}^{n,t} = S_{\text{BSS,DB,stor}}^{n,\text{ini}} + D^{n,t} - \sum_{h=1}^t N_{\text{BSS,DB,sup}}^{n,h}, \forall n \in G_{\text{BSS}}, t \in \mathcal{T} \quad (21)$$

$$S_{\text{BSS,WB,stor}}^{n,t} = S_{\text{BSS,WB,stor}}^{n,\text{ini}} - D^{n,t} + \sum_{h=1}^t N_{\text{BSS,WB,rec}}^{n,h}, \forall n \in G_{\text{BSS}}, t \in \mathcal{T} \quad (22)$$

In the formula: $S_{\text{BSS,DB,stor}}^{n,\text{ini}}$ and $S_{\text{BSS,WB,stor}}^{n,\text{ini}}$ are the DB and WB inventories of BSS n at the initial time, which can be used to reduce the number of truck trips and waiting times. Specifically, when eVTOL battery swapping demand is low, the BSS can directly use $S_{\text{BSS,WB,stor}}^{n,\text{ini}}$ to meet the demand without scheduling trucks. When a truck arrives at the BSS, if the DBs generated from service are insufficient, it can directly load DBs from $S_{\text{BSS,DB,stor}}^{n,\text{ini}}$, thereby shortening waiting times.

Similarly, the quantities of batteries loaded, unloaded, and inventoried at BSS n must also be constrained within reasonable ranges. The corresponding constraints are as follows:

$$\left. \begin{aligned} 0 \leq N_{\text{BSS,DB,sup}}^{n,t} &\leq N_{\text{tru}} C_{\text{tru,cap}}, \forall n \in G_{\text{BSS}}, t \in \mathcal{T} \\ 0 \leq N_{\text{BSS,WB,rec}}^{n,t} &\leq N_{\text{tru}} C_{\text{tru,cap}}, \forall n \in G_{\text{BSS}}, t \in \mathcal{T} \\ 0 \leq S_{\text{BSS,DB,stor}}^{n,t} &\leq 800, \forall n \in G_{\text{BSS}}, t \in \mathcal{T} \\ 0 \leq S_{\text{BSS,WB,stor}}^{n,t} &\leq 800, \forall n \in G_{\text{BSS}}, t \in \mathcal{T} \end{aligned} \right\} \quad (23)$$

In the formula: N_{tru} is the number of all trucks in the BCSS.

To facilitate the BCSS in initiating operations for the next cycle, at the end of each operational cycle, the WB and DB inventories of BSS n should return to their initial levels. That is, the deviation between the battery inventory at the final time step and the initial inventory must not exceed ε batteries. This constraint can be described as:

$$\left| S_{\text{BSS,DB,storage}}^{n,T} - S_{\text{BSS,DB,storage}}^{n,\text{ini}} \right| \leq \varepsilon, \forall n \in G_{\text{BSS}} \quad (24)$$

$$\left| S_{\text{BSS,WB,storage}}^{n,T} - S_{\text{BSS,WB,storage}}^{n,\text{ini}} \right| \leq \varepsilon, \forall n \in G_{\text{BSS}} \quad (25)$$

3) BSS Objective Function

The objective of the BSS is to maximize its operational revenue by optimizing the quantity of WBs it receives, the quantity of DBs it provides, and its dynamic inventory. Its objective function is as follows:

$$\max P_{\text{obj,BSS}} = \eta_{\text{batt_swap}} \sum_{n \in G_{\text{BSS}}} D^{n,T} \quad (26)$$

In the formula: $\eta_{\text{batt_swap}}$ is the revenue obtained from providing one battery swapping service.

C. BCS Operation Model

Building on the integrated consideration of the logistics system model, the BSS operational model, and the operational characteristics of the BCS, this paper constructs an operational model for the BCS. This section elaborates further on core aspects of this model, including the dynamic battery inventory, charging energy, and charging power.

1) BCS Battery Dynamic Inventory Model

Equation (27) provides the definition of $N_{BCS,DB,rec}^{m,t}$, which is the quantity of DBs received by BCS m from the logistics system at time step t . It is the sum of DBs unloaded by all trucks parked at this BCS:

$$N_{BCS,DB,rec}^{m,t} = \sum_{\omega} N_{tru,BCS,DB}^{\omega,m,t}, \forall \omega \in H, \forall m \in G_{BCS}, t \in \mathcal{T} \quad (27)$$

Similarly, the quantity of WBs, denoted as $N_{BCS,WB,sup}^{m,t}$, provided by BCS m to the logistics system can be defined as:

$$N_{BCS,WB,sup}^{m,t} = \sum_{\omega} N_{tru,BCS,WB}^{\omega,m,t}, \forall \omega \in H, \forall m \in G_{BCS}, t \in \mathcal{T} \quad (28)$$

Let $N_{BCS,bin}^{m,t}$ be the number of batteries placed into charging piles by BCS m at time step t , and $N_{BCS,bout}^{m,t}$ be the number of batteries taken out from charging piles. Therefore, the number of batteries in the charging piles of BCS m at time step t can be expressed as:

$$S_{BCS,in_char}^{m,t} = \sum_{h=1}^t N_{BCS,bin}^{m,h} - \sum_{h=1}^t N_{BCS,bout}^{m,h}, \forall m \in G_{BCS}, t \in \mathcal{T} \quad (29)$$

Let $N_{BCS,back}^{m,t}$ first denote the quantity of backup DBs deployed by BCS m at time step t . Combining Equations (27), (28), and (29), the DB inventory $S_{BCS,DB,stor}^{m,t}$ and WB inventory $S_{BCS,WB,stor}^{m,t}$ of the BCS can be derived as follows:

$$S_{BCS,DB,stor}^{m,t} = \sum_{h=1}^t (N_{BCS,back}^{m,h} + N_{BCS,DB,rec}^{m,h} - N_{BCS,bin}^{m,h}), \forall m \in G_{BCS}, t \in \mathcal{T} \quad (30)$$

$$S_{BCS,WB,stor}^{m,t} = \sum_{h=1}^t (N_{BCS,bout}^{m,h} - N_{BCS,WB,sup}^{m,h}), \forall m \in G_{BCS}, t \in \mathcal{T} \quad (31)$$

To ensure the completeness of the battery charging process, a minimum charging time constraint must be introduced. Constraint (32) prevents the charging process from being prematurely interrupted, thereby ensuring that each battery can reach a usable state of charge.

$$\sum_{h=1}^t N_{BCS,bout}^{m,h} \leq \sum_{h=1}^{t-(T_c-1)} N_{BCS,bin}^{m,h}, \forall m \in G_{BCS}, t \in \mathcal{T} \quad (32)$$

In the formula: T_c is the minimum time required to fully charge a battery.

All decision variables of the BCS must also remain within reasonable bounds. Their expressions can be formulated as:

$$\left. \begin{aligned} 0 &\leq N_{BCS,bin}^{m,t} \leq N_{charge}, \forall m \in G_{BCS}, t \in \mathcal{T} \\ 0 &\leq N_{BCS,bout}^{m,t} \leq N_{charge}, \forall m \in G_{BCS}, t \in \mathcal{T} \\ 0 &\leq N_{BCS,back}^{m,t} \leq 1000, \forall m \in G_{BCS}, t \in \mathcal{T} \\ 0 &\leq N_{BCS,DB,rec}^{m,t} \leq N_{tru} C_{tru,cap}, \forall m \in G_{BCS}, t \in \mathcal{T} \\ 0 &\leq N_{BCS,WB,sup}^{m,t} \leq N_{tru} C_{tru,cap}, \forall m \in G_{BCS}, t \in \mathcal{T} \\ 0 &\leq S_{BCS,in_char}^{m,t} \leq N_{charge}, \forall m \in G_{BCS}, t \in \mathcal{T} \\ 0 &\leq S_{BCS,DB,stor}^{m,t} \leq 1000, \forall m \in G_{BCS}, t \in \mathcal{T} \\ 0 &\leq S_{BCS,WB,stor}^{m,t} \leq 1000, \forall m \in G_{BCS}, t \in \mathcal{T} \end{aligned} \right\} \quad (33)$$

In the formula: N_{charge} is the number of charging piles at the BCS, set to 300 charging piles.

Furthermore, certain restrictions must be imposed on the time steps and quantities concerning the WBs taken out from the charging piles by the BCS and the WBs supplied to the logistics system:

$$\left. \begin{aligned} N_{BCS,bout}^{m,t} &= 0, \forall m \in G_{BCS}, t = 1 \\ N_{BCS,bout}^{m,t} &\leq S_{BCS,in_char}^{m,t-1}, \forall m \in G_{BCS}, t \in \mathcal{T} \setminus \{1\} \end{aligned} \right\} \quad (34)$$

Equation (34) stipulates that WBs can only be taken out from the charging piles starting from time step 2, and the quantity taken out cannot exceed the total number of batteries in the charging piles at the previous time step. Equation (35) stipulates that the BCS cannot supply WBs to the logistics system at time step 1. At other time steps, it may supply WBs, but the quantity must not exceed the WB inventory of the BCS at the previous time step.

$$\left. \begin{aligned} N_{BCS,WB,supply}^{m,t} &= 0, \forall m \in G_{BCS}, t = 1 \\ N_{BCS,WB,supply}^{m,t} &\leq S_{BCS,WB,storage}^{m,t-1}, \forall m \in G_{BCS}, t \in \mathcal{T} \setminus \{1\} \end{aligned} \right\} \quad (35)$$

2) Energy and Power Constraints of the BCS

The operation of the BCS must consider the cost of electricity procurement. To control this cost, it must be ensured that all energy consumed by BCS m is used for battery charging. The corresponding expression is as follows:

$$\sum_{h=1}^t (P_{\text{BCS, char}}^{m,h} \alpha_{\text{effi, char}} \Delta t) = E_{\text{batt, en}} \sum_{h=1}^t N_{\text{BCS, bout}}^{m,h}, \forall m \in G_{\text{BCS}}, t \in \mathcal{T} \quad (36)$$

In the formula: $P_{\text{BCS, char}}^{m,t}$ is the total charging power supplied by BCS m at time step t , which is the sum of the charging power required by all batteries being charged; $\alpha_{\text{effi, char}}$ is the charging efficiency; $E_{\text{batt, en}}$ is the single battery capacity.

For $P_{\text{BCS, char}}^{m,t}$ in Equation (36), Equation (37) defines its adjustable range during optimization:

$$0 \leq P_{\text{BCS, char}}^{m,t} \leq P_{\text{max, char}} N_{\text{charge}} \beta_{\text{BCS, char, sign}}^{m,t}, \forall m \in G_{\text{BCS}}, t \in \mathcal{T} \quad (37)$$

In the formula: $P_{\text{max, char}}$ is the maximum charging power that each charging pile can supply to a battery; $\beta_{\text{BCS, char, sign}}^{m,t}$ is a binary variable indicating the charging status of BCS m , taking the value 1 if the BCS is permitted to charge, and 0 otherwise.

3) BCS Objective Function

The primary objective of the BCS is to meet the WB demand of BSSs while adhering to all operational constraints. Under this premise, to maximize operational revenue, the BCS must formulate an optimal operational strategy by optimizing the timing of electricity procurement, the magnitude of charging power, and the quantity of backup DBs used. Its objective function is as follows:

$$\max P_{\text{obj, BCS}} = \sum_{m \in G_{\text{BCS}}} \sum_{t=1}^T [-(\lambda_{\text{pri, mark}}^t + \lambda_{\text{pri, batt}}) P_{\text{BCS, char}}^{m,t} - \lambda_{\text{pri, back}} N_{\text{BCS, back}}^{m,t}], \forall t \in \mathcal{T} \quad (38)$$

In the formula: The first term is the sum of the total electricity procurement cost and the total battery degradation compensation cost due to charging over T time steps. The second term is the total cost incurred from deploying backup DBs, which refers to the fees paid by the BCS to a third-party company for leasing batteries when it urgently needs to meet the BSS's WB demand but finds its own DB inventory insufficient. $\lambda_{\text{pri, mark}}^t$ is the electricity procurement unit price at

time step t ; $\lambda_{\text{pri, batt}}$ is the unit price for compensating battery degradation; $\lambda_{\text{pri, back}}$ is the cost of deploying a backup DB.

Integrating all the models above, this paper establishes the following total objective function and operational constraints for the BCSS to achieve optimal system scheduling. Since the research problem constitutes a mixed-integer linear programming problem, the commercial solver Gurobi is employed to solve it using a centralized method.

$$\left. \begin{aligned} \max P_{\text{obj, all}} &= P_{\text{obj, tran}} + P_{\text{obj, BSS}} + P_{\text{obj, BCS}} \\ \text{s.t.} & (1)-(15), (17)-(25), (27)-(37). \end{aligned} \right\} \quad (39)$$

IV. CASE STUDY

To validate the effectiveness of the eVTOL battery charging and swapping system model based on CLSC and TSN proposed in this paper, this section conducts a simulation analysis for the scenario illustrated in Fig. 1. The case study is programmed using MATLAB R2022b, and the commercial solver Gurobi is called for the solution.

In the simulation, the BCSS managed by the eVTOL operator consists of several eVTOLs requiring battery swapping, four trucks, three BSSs, and one BCS. The operational cycle T is set to twenty-four time steps, with the objective of maximizing the comprehensive operational revenue of the entire system. All four trucks are located at the BCS at the initial time step. The $A^{n,t}$ and $D_{\text{min}}^{n,t}$ for each BSS at each time step are shown in Fig.4. The electricity procurement prices during the operational cycle are sourced from data published by Singapore's EMC^[25] on December 15, 2017, as shown in Fig. 5. The remaining simulation parameters are summarized in Table I.

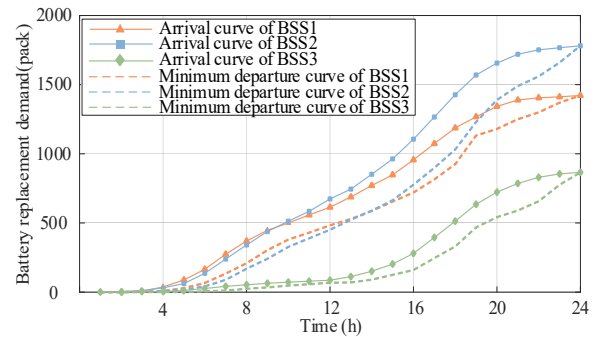


Fig. 4. Arrival curve and minimum departure curve of BSSs.

The solution time and key operational results of the BCSS are presented in Table II. To thoroughly evaluate the system performance, the simulation results of the logistics system operational model, the BSS operational model, and the BCS operational model will be analyzed and discussed separately.

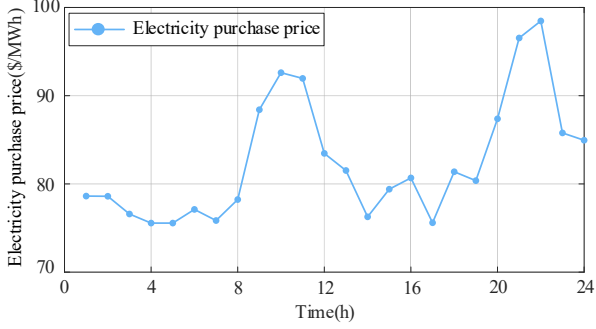


Fig. 5. Electricity purchase price of BCS.

TABLE I. PARAMETERS OF BCSS

Parameter Name	Value	Parameter Name	Value
$C_{tru,cap}$ (pack)	300	$\lambda_{pri,back}$ (\$/pack)	5
$\lambda_{tru,tran}$ (\$/h)	10	$\lambda_{pri,batt}$ (\$/kWh)	0.01
λ_{labor} (\$/pack)	0.1	$E_{batt,en}$ (kWh)	30
$S_{BSS,DB,stor}^{n,ini}$ (pack)	200	$\alpha_{effi,char}$	0.95
$S_{BSS,WB,stor}^{n,ini}$ (pack)	200	ε (pack)	30
η_{batt_swap} (\$/pack)	6	$P_{max,char}$ (kW)	120

TABLE II. OPERATIONAL RESULTS OF BCSS

$P_{obj,tran}$	$P_{obj,BSS}$	$P_{obj,BCS}$	Solution Time
-2021.6 \$	24414 \$	-16059.82 \$	10129.79 s

A. Analysis of Logistics System Simulation Results

Fig. 6-9 respectively present the scheduling results of the four trucks during the operational cycle, validating the effectiveness of the proposed logistics system model. In Fig. 6(a), 7(a), and 9(a), Truck1, Truck2, and Truck4 each proceed to different BSSs in the initial few time steps and return with a large number of DBs. This strategy reduces the quantity of

backup DBs that the BCS needs to deploy, effectively lowering operational costs. The scheduling strategy for Truck3 differs, as shown in Fig. 8(b). It waits at the BCS for 3 time steps, loads WBs only at time step4, and then proceeds to BSS1. Furthermore, as seen in Fig. 6, Truck1 does not rush to unload DBs to the BCS at time step4 but first loads 79 WBs. Therefore, loading before unloading is permitted as long as the sum of the batteries already on the truck and the batteries to be loaded in this operation does not exceed the truck's maximum battery capacity. This practice makes full use of the truck's space, alleviates the battery storage pressure on the stations to some extent, and also increases the BCSS's flexibility in truck scheduling. The scheduling results of the logistics system also indicate that when a truck is parked at a station, it can load and unload a large number of batteries within a single time step, provided unloading occurs before loading to ensure the number of batteries on board never exceeds the maximum capacity.

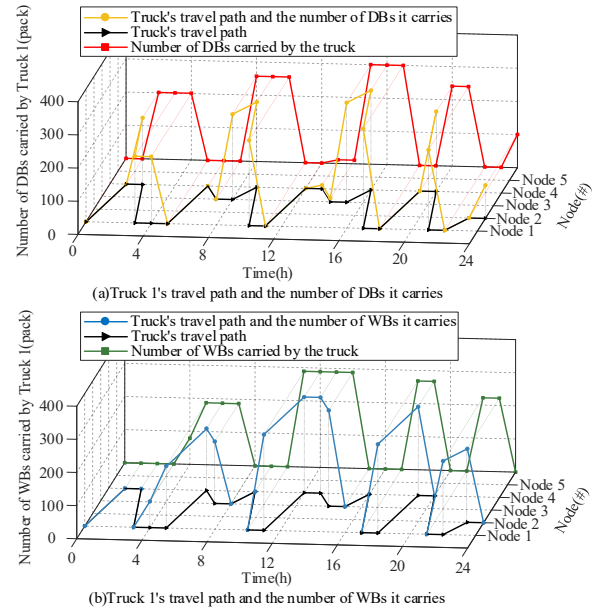


Fig. 6. Driving trajectory and change in battery inventory of Truck1.

Fig. 4 indicates that the battery swapping demand at BSS1 and BSS2 is significantly higher than that at BSS3, which is the primary factor determining the travel routes of the four trucks. The main service target of Truck2 is BSS2; it only occasionally stops at BSS1 and BSS3 to load or unload batteries while passing by. The main service target of Truck4 is BSS1,

operating exclusively between the BCS and BSS1 from time step 1 to 20. The travel route of Truck1 primarily involves moving among BSS2, BSS3, and the BCS, only stopping at BSS1 for battery operations at the final time step. The scheduling of Truck3 is more balanced, covering all BSS in its service scope. This indicates that the WB demand of BSS3 is met jointly by Truck1 and Truck3. Furthermore, Trucks2-4 all remain at BSS2 at the last time step, and the DBs they carry are all provided by that BSS.

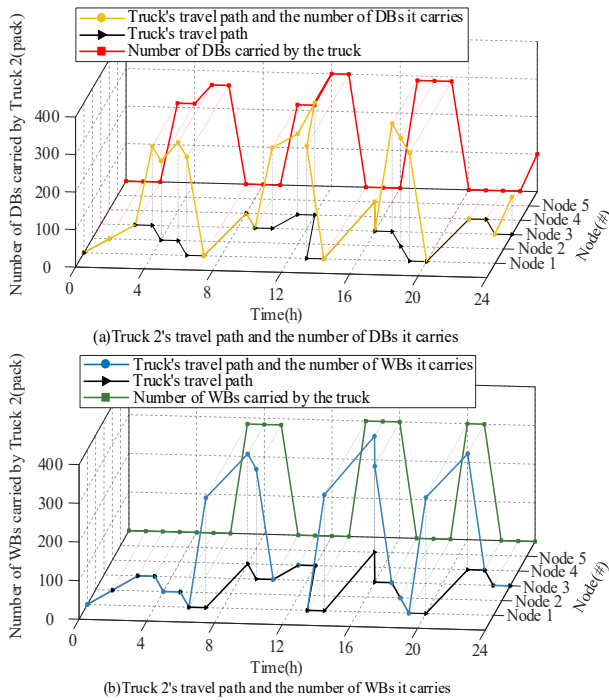


Fig. 7. Driving trajectory and change in battery inventory of Truck2.

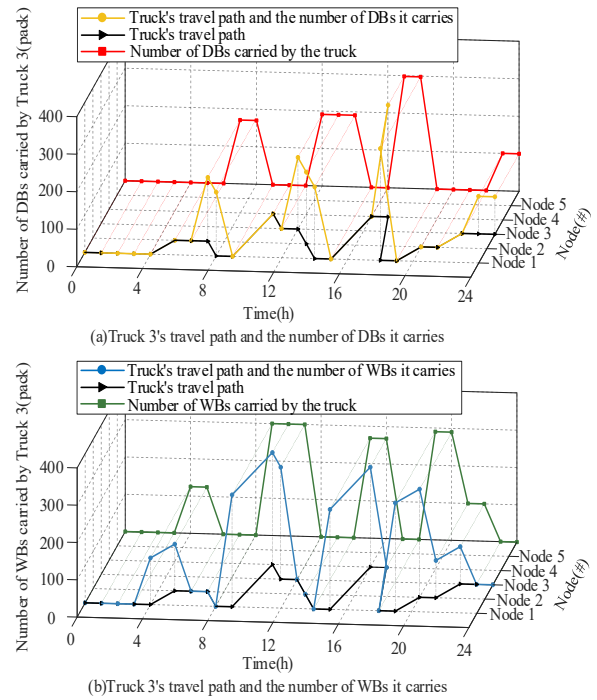


Fig. 8. Driving trajectory and change in battery inventory of Truck3.

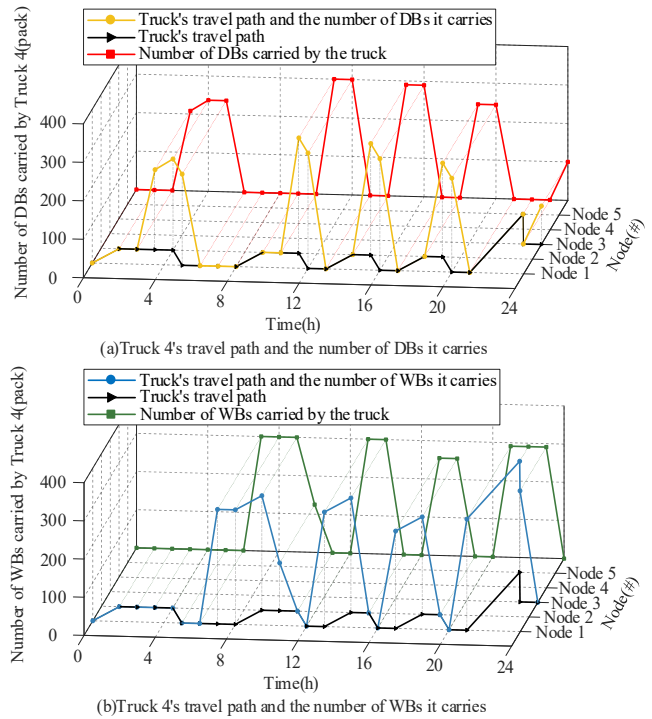


Fig. 9. Driving trajectory and change in battery inventory of Truck4.

B. Analysis of BSS Simulation Results

Combining Fig. 4 and Fig. 10, it can be observed that the battery swapping demand for all BSSs is relatively low during time steps 1-6, and each BSS has an initial WB inventory.

Consequently, the $D^{n,t}$ of each BSS largely aligns with its $A^{n,t}$. By jointly examining Fig. 4, 10, and 11, it is found that BSS1 exhibits the phenomenon of maintaining a small WB inventory. For instance, during time steps 13, 14, 16, 17, and 22, BSS1 has WB inventory but does not perform battery swapping. Furthermore, when the $D^{n,t}$ and $D_{\min}^{n,t}$ of BSS1 are equal, the system rapidly delivers a large quantity of WBs in subsequent time steps. For example, after swapping at time step 9, the $D^{n,t}$ of BSS1 equals its $D_{\min}^{n,t}$. Subsequently, Truck4 unloads 300 WBs to BSS1 in batches during time steps 10 and 11. Throughout the operational cycle of BSS1, its $D^{n,t}$ equals $A^{n,t}$ and $D_{\min}^{n,t}$ on multiple occasions. Analysis reveals that BSS1 has a large $A^{n,t}$ and must strictly adhere to the $D_{\min}^{n,t}$ constraint. However, the frequency of truck service arranged by the logistics system for BSS1 is lower than that for BSS2, leading to repeated occurrences of extreme operating conditions and the maintenance of a small WB inventory.

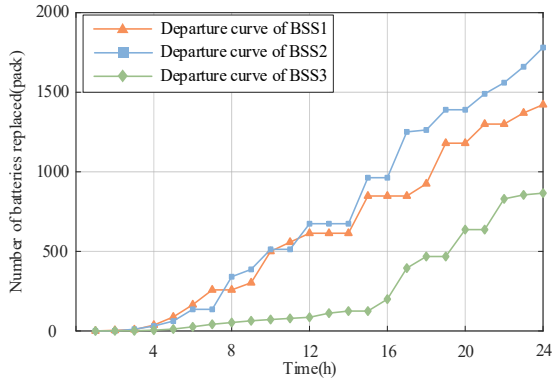


Fig. 10. Battery-swap result of the BSS Model.

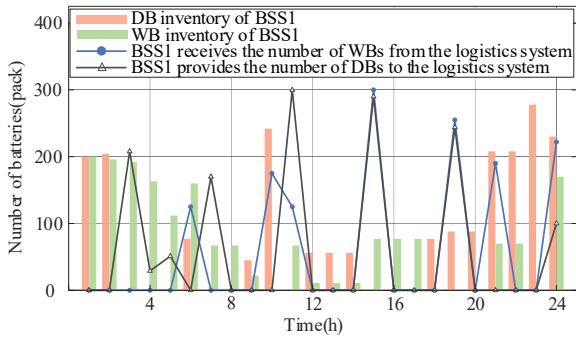


Fig. 11. Operational results of BSS1.

As shown in Fig. 10 and 12, BSS2 also exhibits situations at time steps 7, 11, 13, and 14 where it does not provide battery swapping services despite having WB inventory, yet its $D^{n,t}$ remains within a reasonable range. At time steps 15 and 17, the system replenished this BSS with a large number of WBs via trucks. Combined with its existing WB inventory, this resulted in the BSS maintaining a high WB inventory level during time steps 15-18, regardless of the actual number of battery swaps. Due to the absence of WB replenishment from time step 18 to 22, BSS2 was forced to reduce its $D^{n,t}$ to $D_{\min}^{n,t}$ from time step 20 to 22 and ultimately depleted its WB inventory. Although this BSS received 100 WBs at time step 23, it was insufficient to alleviate the backlog of swapping demand, and it was not until time step 24 that all battery swapping targets for the operational cycle were completed. Overall, despite handling the largest battery swapping demand, the WB supply for BSS2 was sufficient for most of the time, allowing its operation to remain smooth and manageable from time step 1 to 19.

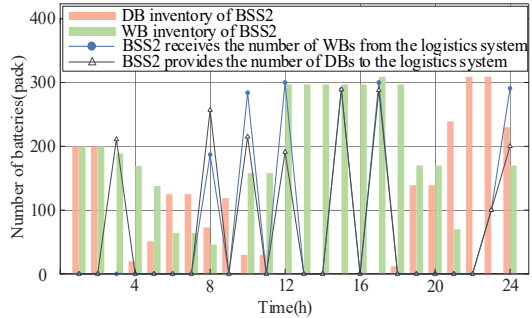


Fig. 12. Operational results of BSS2.

As shown in Fig. 13, despite not receiving any WBs from the logistics system during the first 13 time steps, BSS3 had a relatively low battery swapping demand and, by relying solely on its initial WB inventory, was able to keep its $D^{n,t}$ nearly consistent with its $A^{n,t}$ during this period. Within the first 11 time steps, BSS3 only supplied 201 DBs to the logistics system at time step 2. BSS3 experienced fewer instances where its $D^{n,t}$ equaled its $D_{\min}^{n,t}$. Even when such situations occurred, trucks would promptly arrive to deliver WBs and collect all DBs, and could even leave a certain WB inventory at this BSS, as seen at

time step17. Throughout the entire operational cycle, BSS3 delivered DBs to the logistics system only 5 times, significantly lower in both frequency and quantity compared to the other BSS. Furthermore, it is evident that the WB inventory of each BSS is updated only after receiving WBs from the logistics system and completing the battery swapping service for that time step, while the DB inventory is updated only after the swapping service concludes and the DBs are provided to the logistics system.

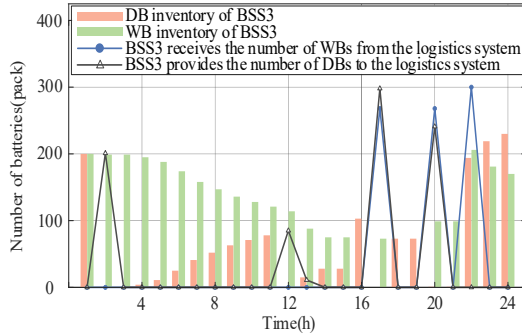


Fig. 13. Operational results of BSS3.

C. Analysis of BCS Simulation Results

As shown in Fig. 14, at any given time step, if the BCS deploys backup DBs or unloads DBs from trucks, it is permissible to place these batteries into the charging piles immediately within the same time step. When investigating the variation pattern of the DB inventory at this BCS, it is necessary to comprehensively consider a series of decision variables, including the quantity of backup DBs deployed, the quantity of DBs unloaded from trucks, and the quantity of DBs placed into charging piles. Fig. 15 illustrates the WB inventory update mechanism of the BCS, which responds to updates only after the BCS withdraws WBs from charging piles and trucks take WBs away. Throughout the entire operational cycle, the BCS deployed backup DBs only 4 times, between time steps2 and 6, with a cumulative total of 958 batteries.

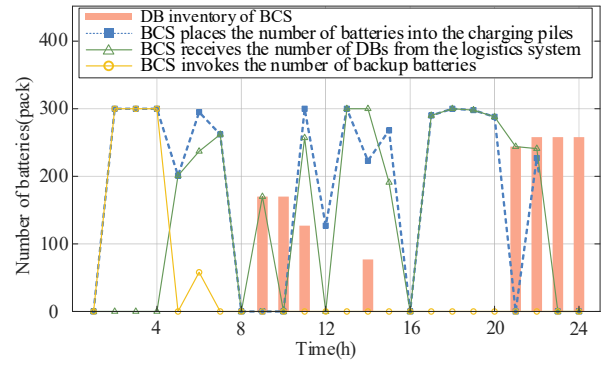


Fig. 14. BCS's DB inventory and its related variables.

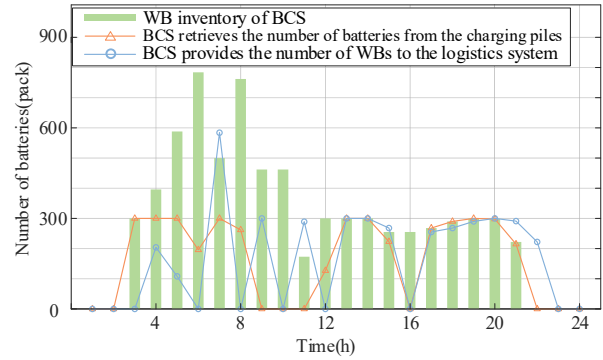


Fig. 15. BCS's WB inventory and its related variables.

Combining Fig. 5 and 14, it can be observed that, given that electricity prices during time steps9-11 are in a higher range, the BCS did not place any DBs into charging piles at time steps9 and 10. Even though 300 DBs were placed at time step11, they were not charged. From Fig. 15, it is noted that the BCS withdrew only 127 WBs at time step12. The reason is that while electricity price at this time had declined compared to those in time steps 9-11, it remained higher than the price levels during time steps 1-8 and 13-19. Although electricity prices in time steps20-21 increased significantly compared to earlier periods, the BCS had to charge batteries during these peak-price periods to meet the WB demand of BSSs. Nonetheless, only some batteries in the charging piles were charged at time step21. During time steps22-24, the number of batteries in the charging piles remained constant at 300, while the WB inventory of the BCS stayed at 0. This is because the electricity procurement prices during this phase were excessively high, and the cumulative WBs provided in the first 21 time steps were already

sufficient to fully meet the battery swapping demand of all BSSs. Therefore, the BCS ceased charging batteries.

V. CONCLUSION

This paper addresses the issue of rapid energy replenishment for eVTOL batteries by proposing a CLSC-based model for the eVTOL battery charging and swapping system. With the objective of maximizing operational revenue, it optimizes the management of all members within the system. Finally, the feasibility of the proposed model is validated through simulation, filling the gap in the integrated operation and management of eVTOLs, BSSs, and BCSs. The following conclusions are drawn:

(1) The eVTOL battery charging and swapping system model proposed in this paper, by decoupling the battery swapping strategy from centralized charging, not only leverages the numerous advantages of battery swapping over plug-in charging, but also effectively overcomes the inherent drawbacks of BSS operating independently, thereby establishing a highly efficient and synergistic rapid energy replenishment system.

(2) The model in this paper clearly defines the functions of each member within the system: the logistics system optimizes battery transportation routes and loading/unloading quantities based on global operational demands; BSSs consider both battery inventory and eVTOL swapping needs to formulate reasonable swapping plans that balance service quality and operational costs; the BCS, while meeting BSSs' demands and coordinating logistics, reduces operational costs by dynamically deploying backup DBs and optimizing charging strategies. The synergistic operation of these three components ensures the overall economic efficiency and high performance of the system.

(3) The simulation results in this paper demonstrate that this integrated operational model can not only alleviate the range constraints of eVTOLs and promote their commercialization but also provide theoretical reference for the sustainable and intelligent evolution of distribution grids. Through centralized battery charging and flexible scheduling, the system can guide the temporal and spatial distribution of charging loads, thereby

flattening peak-valley differences in regional grids and reducing expansion pressure. Furthermore, this model helps advance the coordinated planning of charging infrastructure and distribution grids, enhancing grid flexibility and resilience. In the long term, eVTOL battery clusters can serve as dispatchable distributed energy storage resources to participate in grid interactions, leveraging their potential in demand response, frequency regulation, and other aspects, thereby driving the transformation and upgrade of distribution grids toward intelligence and sustainability.

REFERENCES

- [1] SHANGHAI CPPCC. The 35th standing committee meeting of the 13th Shanghai CPPCC[EB/OL]. (2022-07-06)[2025-09-25].<https://www.shszx.gov.cn/shzx/hyjj/content/ac2382f3-340a-44d0-a7fb-201889ca1b95.html>.
- [2] MORGAN STANLEY.eVTOL/urban air mobility TAM update:a slow take-off,but sky's the limit[R/OL]. (2021)[2025-09-25].<https://advisor.morganstanley.com/the-busot-group/documents/field/b/bu/busot-group/Electric%20Vehicles.pdf>.
- [3] M. Wang, G. Xiaoyang, R. He, S. Zhang, and J. Ma, "Bi-layer sizing and design optimization method of propulsion system for electric vertical takeoff and landing aircraft," *Energy*, vol. 283, p. 129052, 2023.
- [4] J. He et al., "Key technologies and upgrade strategies for eVTOL aircraft energy storage systems," *Journal of Energy Storage*, vol. 103, p. 114402, 2024.
- [5] X. Yang, T. Liu, S. Ge, E. Rountree, and C. Wang, "Challenges and key requirements of batteries for electric vertical takeoff and landing aircraft," *Joule*, vol. 5, no. 7, pp. 1644–1659, 2021.
- [6] A. Singh, A. Lodge, Y. Li, W. D. Widanage, and A. Barai, "A new method to perform lithium-ion battery pack fault diagnostics – Part 3: Adaptation for fast charging," *Journal of Energy Storage*, vol. 66, p. 107424, 2023.
- [7] C. Y. Justin, A. P. Payan, S. I. Briceno, B. J. German, and D. N. Mavris, "Power optimized battery swap and recharge strategies for electric aircraft operations," *Transportation Research Part C: Emerging Technologies*, vol. 115, p. 102605, 2020.
- [8] J. Park, D. Lee, D. Lim, and K. Yee, "A refined sizing method of fuel cell-battery hybrid system for eVTOL aircraft," *Applied Energy*, vol. 328, p. 120160, 2022.
- [9] Z. Wu and Y. Zhang, "Optimal eVTOL charging and passenger serving scheduling for on-demand urban air mobility," *Vertical/Short Take-Off and Landing (V/STOL) Aircraft Systems : AIAA Aviation Forum*, 15-19 June 2020, pp. 1–8, 2020.

- [10] J. Chen, "Integrated routing and charging scheduling for autonomous electric aerial vehicle system," 2019 IEEE/AIAA 38th Digital Avionics Systems Conference (DASC), pp. 1–7, 2019.
- [11] J. Wu, S. Cao, M. Hansen, and M. C, "Integrating urban air mobility into the power grid through smart charging solutions," *Transportation Research Part C: Emerging Technologies*, vol. 179, p. 105281, 2025.
- [12] Z. Guo, B. Li, G. Taylor, and X. Zhang, "Infrastructure planning for airport microgrid integrated with electric aircraft and parking lot electric vehicles," *eTransportation*, vol. 17, p. 100257, 2023.
- [13] M. Liu et al, "Exploring the key technologies needed for the commercialization of electric flying cars: A leveled cost and profitability analysis," *Energy*, vol. 303, p. 131991, 2024.
- [14] N. A. El-Taweel, A. Ayad, H. E. Z. Farag and M. Mohamed, "Optimal energy management for battery swapping based electric bus fleets with consideration of grid ancillary services provision," *IEEE Transactions on Sustainable Energy*, vol. 14, no. 2, pp. 1024-1036, April 2023.
- [15] X. Liu, T. Zhao, S. Yao, C. B. Soh, and P. Wang, "Distributed operation management of battery swapping-charging systems," *IEEE Transactions on Smart Grid*, vol. 10, no. 5, pp. 5320–5333, 2019.
- [16] X. Zhang, G. Wang, "Optimal dispatch of electric vehicle batteries between battery swapping stations and charging stations," 2016 IEEE Power and Energy Society General Meeting (PESGM), pp. 1–5, 2016.
- [17] Z. Miao, K. Fu, Z. Xia, and Y. Wang, "Models for closed-loop supply chain with trade-ins," *Omega*, vol. 66, pp. 308–326, 2017.
- [18] H. Chu, W. Zhang, and L. Zhu, "The impact of government policies on the coordination of power battery closed-loop supply chain," *Journal of Cleaner Production*, vol. 519, p. 145961, 2025.
- [19] M. Tavana, H. Kian, A. K. Nasr, K. Govindan, and H. Mina, "A comprehensive framework for sustainable closed-loop supply chain network design," *Journal of Cleaner Production*, vol. 332, p. 129777, 2022.
- [20] S. Yao, P. Wang and T. Zhao, "Transportable Energy Storage for More Resilient Distribution Systems With Multiple Microgrids," *IEEE Transactions on Smart Grid*, vol. 10, no. 3, pp. 3331-3341, May 2019.
- [21] P. Lin, L. Du, H. Zhang, M. Zhu, J. Ma, and P. Wang, "Power lever: To transform interlinking architecture in hybrid ac/dc microgrids community," *IEEE Transactions on Industrial Electronics*, 2025.
- [22] P. Lin, Q. Meng, M. Zhu, A. M. Y. M. Ghias, and F. Blaabjerg, "Dynamic circuit-based unified power regulation for hybrid ac/dc/ds microgrids: A comprehensive approach to static and transient control," *IEEE Transactions on Industrial Electronics*, 2025.
- [23] X. Liu, C. B. Soh, T. Zhao and P. Wang, "Stochastic Scheduling of Mobile Energy Storage in Coupled Distribution and Transportation Networks for Conversion Capacity Enhancement," *IEEE Transactions on Smart Grid*, vol. 12, no. 1, pp. 117-130, Jan. 2021.
- [24] M. A. Zafer and E. Modiano, "A calculus approach to energy-efficient data transmission with quality-of-service constraints," *IEEE/ACM Transactions on Networking*, vol. 17, no. 3, pp. 898–911, 2009.
- [25] EMC Market Data. [Online]. Available: <https://www.emcsg.com>